Performance Assessment of Bladeless Micro-Expanders Using 3D Numerical Simulation

Avinash Renuke[1,*], *Alberto Traverso*[1] , and *Matteo Pascenti*[2]

[1]Thermochemical Power Group (TPG), University of Genoa, Italy
[2]SIT Technologies, Italy

Abstract. This paper summarizes the development of fully 3D Computational Fluid Dynamics (CFD) analysis for bladeless air micro expander for 200 W and 3 kW rated power. Modelling of nozzle along with rotor is done using structured mesh. This analysis, for the first time, demonstrates the interaction between nozzle and rotor using compressible flow density-based solver. The Shear Stress Transport (SST) turbulence model is employed to resolve wall effects on the rotor and to determine the shear stress accurately. The results illustrate the flow field inside stator and rotor along with complicated mixing zone between stator and rotor. The comparison of rotor-stator CFD simulation results is done with experiments to preliminary validate the model. The losses in the turbine are discussed with the help of experimental and numerical data.

1 Introduction

This paper focuses on prediction, validation and investigation of performance of Tesla type turbines for micro power generation, using Computational Fluid Dynamic (CFD) analysis. The experiment campaign is run in Thermochemical Power Group (TPG), University of Genoa, Italy for Tesla expanders of 200W (M02) [1] and 3 kW (M3) design power fed by air. The CFD results of these two turbines are compared with experimental data to validate the model and characterize the losses.

The bladeless turbomachinery, also known as multiple disk turbines or Tesla turbines, was invented by Nikola Tesla in 1913 [2,3]. It consists of an array of parallel thin disks very close to each other, separated by spacers and assembled on a shaft, forming a rotor which is fitted in a cylindrical housing with its ends closed by plates properly fitted with bearings to hold the rotor shaft. Fluid enters tangentially into the turbine from stator. The momentum of the moving fluid is transferred to disks because of viscosity and adhesion. The friction force generated by the fluid transfers this momentum to the disks. Many researchers have performed experimental activities [1] on Tesla micro turbines and modified it to enhance its performance.

A three-dimensional computational fluid dynamic (CFD) analysis of Tesla turbine initially appears in work done by Ladino [4,5] with air as a working fluid. Geometry is modelled with two simple, constant section nozzles. Maximum efficiency of around 20% has

* Corresponding author: avinash.renuke@edu.unige.it

been predicted. Lemma et al [6] performed experimental and numerical study on a 50 mm rotor Tesla turbine. The results of experimental study indicate that the adiabatic efficiency of these machines is around 25%. The main reasons for the low efficiency have been identified to be parasitic losses in the bearing and viscous losses in the end walls. The parasitic losses are about 92% of the measured load. Bearing losses are suspected as the main cause of these losses. Lampart et al [7] developed a CFD investigation on different Tesla turbine dimensions with SES36 (Fluent database) as working fluid. The predicted efficiency of turbine oscillates around 50%. Rusin et al [8] compared the experimental results of Tesla turbine with numerical analysis by considering the surface roughness of the disks. The highest power and efficiency values obtained were: 55.6 W, 11.2% for inlet pressure 3 bar and 98.3 W, 11.8% for 4 bar. Qi et al [9] performed the numerical analysis to investigate the influence of disk tip geometry on the performance of Tesla turbine.

There is no clear assessment of loss characterization and contribution of each component towards performance of the Tesla turbine using CFD simulation. A simplified nozzle (hole with constant diameter) has been used in the past work. This paper presents the CFD simulation with Convergent-Divergent (CD) nozzle and Convergent only nozzle analysis. This paper mainly discusses effect of CD and convergent only nozzles on the performance of turbine. The numerical analysis is performed using a commercially available CFD software Ansys 19.2 version. Fluent, a finite volume solver which is part of Ansys, is used to solve Navier-Stokes equations.

2 Geometries and computational setup

Two turbines, M02 and M3, with different nozzle configuration and design power output has been investigated. Table 1 shows the geometrical parameters of both the turbine models which are tested and for which CFD models are created. M02 turbine has eight convergent divergent nozzles with design power of 200 W. M3 turbine has eight convergent nozzles with design power of 3 kW. M03 is improved version which is designed based on lessons learnt on M02 turbine. M03 turbine parts are made with advanced manufacturing methods like 3D printing and with inhouse generator. A complete 3D model of entire turbine is not feasible considering the restrictions on computational time and resources. A partial 3D model is built which consists of: A nozzle, casing, and disk. The models used for this simulation is shown in Fig. 1. In this model, half disk and half gap are simulated. Such configuration greatly reduces computational efforts without compromising on quality of the results. Turbine M02 is modelled with complete periphery with two nozzles adjacent to each other as shown in Fig. 1 (i) while Turbine M3 is modelled with one sector and one nozzle with periodic boundary condition to obtain 8 nozzle effect as shown in Fig. 1(ii). For both the models, symmetry boundary condition is used at the centre of gap and centre of disk.

Table 1. Geometrical parameters for both turbine models

Parameters	M02	M3
Outer diameter of disk, mm	64.5	120
Inner diameter of disks, mm	30	60
Number of nozzles	2	8
Gap between disks, mm	0.2	0.1
Disk thickness, mm	0.2	0.1
Number of disks	10	118
Nozzle angle, degree	2.2	2.2
Type of nozzle	Convergent-Divergent	Convergent

We have used 'mapped hexahedral meshing' for the model using commercial Ansys ICEM 19.2 software. Mesh sensitivity is carried out by changing grid distribution in the stator and rotor. The grid distribution is different in all three coordinates (axial, radial and tangential). The grid distribution in axial direction is non-uniform to capture wall physics accurately. To resolve the viscous sub layer, y+ between 0 to 1 has been maintained. Mesh sensitivity analysis is carried out for both the models as shown in Table 2. We have selected the mesh model for which we see no significant change in the output parameters such as outlet tangential velocity and outlet temperature. The mesh is refined near nozzle and rotor interaction (seen as darker regions in the graphics) to capture the flow phenomenon better. We also observe fine meshing in rotor area which is the result of mesh modelling of nozzle-rotor blocking.

Table 2. Grid sensitivity analysis

Mesh model #	# of Nodes	# of elements	Outlet Total temperature, K	Torque, Nm	velocity outlet, m/s
Grid distribution variation in rotor					
1	2,6E+06	2,7E+06	281,41	0,001533	60,60
4	1,7E+06	1,8E+06	281,45	0,001534	60,60
3	1,4E+06	1,5E+06	281,45	0,001535	59,66
4	4,3E+05	4,7E+05	281,48	0,001539	58,55
Grid distribution variation in stator					
1	4,3E+05	4,7E+05	281,48	0,001539	58,55
2	8,1E+05	8,8E+05	281,58	0,001527	60,72
3	1,1E+06	1,2E+06	281,43	0,001539	60,72

The following boundary conditions are used in the CFD simulation: (a) At the inlets of both the nozzles :Total pressure and Total temperature; (b) At the outlet: zero static pressure; (c) Disks are considered to be rotating wall with no slip condition; (d) Stationary walls of the casing and the nozzles are given no slip wall condition; (e) Symmetry boundary condition at the centre of the gap between disks and at the centre of disk as shown in Fig 1 for both turbine models; (f) periodic boundary condition for M3 model to have eight nozzles.

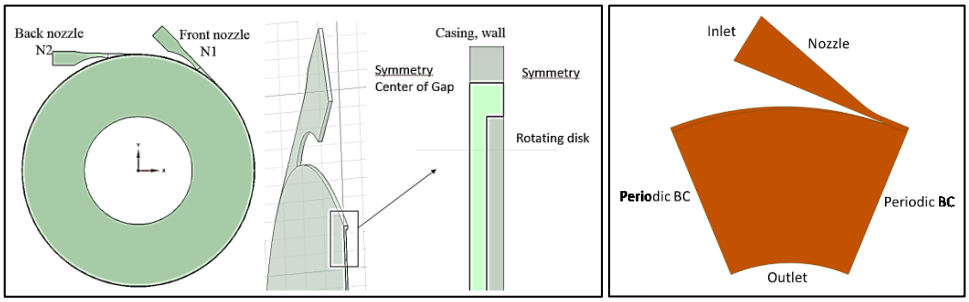

(i) (ii)

Fig. 1. Turbine models: **(i)** M02 turbine model; **(ii)** M3 turbine model

We present CFD simulation for steady, turbulent and compressible supersonic flow. For this purpose, 3D, double precision, density-based solver in Fluent 19.2 is used with energy equation model and transition SST (shear stress transport) to accurately resolve flow at the wall. Compressed air with ideal gas is used as fluid domain. Convergence for residual is tracked till 10^{-6} along with convergence following parameters: outlet tangential velocity, outlet total temperature, torque on disks and mass flux.

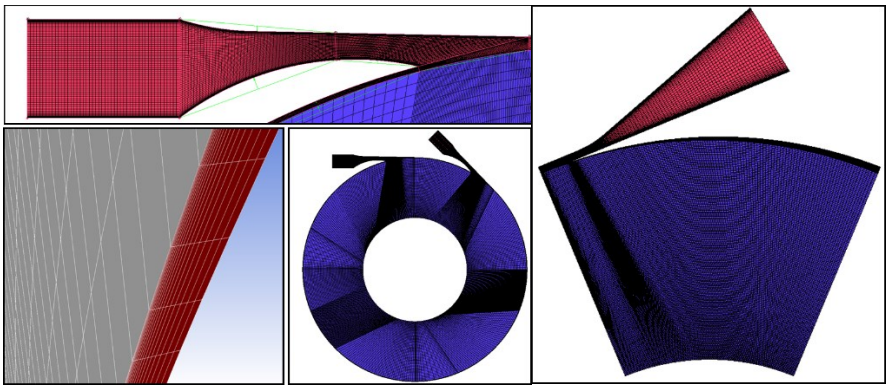

(i) (ii)

Fig. 2. Grid distribution: **(i)** M02 turbine model; **(ii)** M3 turbine model

Performance parameters are calculated based on equations given by Renuke et al [1]. Mechanical power is obtained using torque of the rotor and angular velocity as:

$$P_{cfd} = \tau \cdot \omega \tag{1}$$

Mechanical efficiency of total-to-static $\eta_{cfd.tot.st}$, computed using following expression.

$$\eta_{cfd.tot.st} = \frac{P_{cfd}}{C_p T_{in.tot}\left(1-\frac{1}{\varepsilon^{\frac{k-1}{k}}}\right)\dot{m}} \tag{2}$$

Specific heat at constant pressure, C_p and heat capacity ratio, k is considered constant with temperature. For air, C_p = 1.005 kJ/kg.K and k = 1.4 is used.

The parameter expansion ratio ε is given by,

$$\varepsilon = \frac{p_{in.tot}}{p_{e.st}} \tag{3}$$

3 Results

This section presents the comparison of computational and experimental results for both turbines i.e. M02 and M3.

3.1 Turbine M02

In this section, we compare the experimental and numerical results for M02 turbine. Figure 3 (i) shows the mechanical power calculated using Equ. (1) versus mass flow rate. In CFD model following losses are not considered: (a) entry losses from inlet chamber to inlet of nozzle; (b) leakage through end disks; (c) Viscous friction between end disks and casing) and bearing losses; (d) exhaust duct losses. Ventilation loss and bearing loss are determined by doing run-down test experimentally [1]. This power loss is subtracted from power obtained from CFD analysis. During rundown, peripheral (i.e. in the disk tip clearance) air speed is lower than when nozzles are active. Therefore, we expect that the periphery losses

are much higher when nozzles are activated. CFD is capturing such periphery losses. Therefore, by overlapping the experimentally measured ventilation losses to the CFD results, the result can be conservative. As mentioned by Renuke et al [1], leakages from side disks are evaluated to be around ~ 45 to 50% since the clearance between end disks and casing could not be finely controlled. High-end clearance caused higher leakage across the turbine, hence low power output. Power loss due to leakage has been considered in the calculation of numerical power. As shown in Figure 3, there is good match between CFD and experiment values for mechanical power which validates the CFD model. However, we observe that there is difference in the numerical and experimental results at low mass flow rate. This could be due to the variation of leakage flow at the end disks at different mass flow rate. In the CFD analysis, end leakages are assumed constant for all the turbine mass flow data. Moreover, leakages bypassing the rotor are not experimentally evaluated, in turn they are obtained by fitting other performance parameters in 1D model [1]. A proper prediction of these values and trends represents an object of future investigations.

Figure 3 (ii) shows total to static efficiency versus mass flow rate. Efficiency computed by CFD analysis shows higher values than experimental data. The reason behind mismatch is that the losses due to exhaust and entry losses has not been considered in the CFD analysis results while computing efficiency.

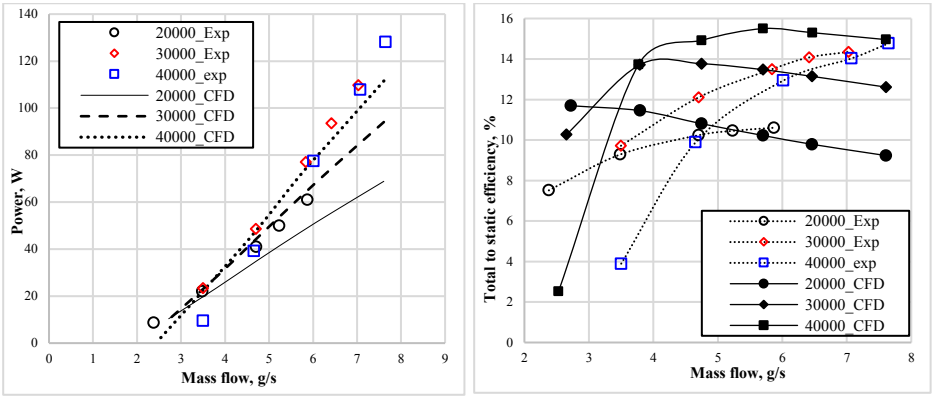

(i) (ii)

Fig. 3. Comparision of CFD and experiment results for M02 turbine : (i) Mechanical power versus mass flow through turbine ; (ii) Total to static efficiency versus mass flow

Numerical analysis shows that the flow is supersonic leading to Mach number of 1.6 at 3.4 bar inlet pressure. The use of convergent-divergent nozzle and the stator-rotor interaction leads to the possibility of the presence of shock waves. The shock waves cause following aerodynamic phenomena: loss of total pressure drop, interaction with other flows such as boundary layer flows to create another flow structure, and sudden change of properties like pressure, Mach number, density, temperature entropy etc. Figure 4 (i) shows the total pressure drop in the divergent section of the nozzle. This tremendous total pressure drop in the nozzle could be due to the strong shock waves created by supersonic flow.

Another interesting aspect to study is the effect on the nozzles when placed adjacent to each other. It is very crucial to select the number of nozzles as it affects the overall performance of the turbine. In this paper, we have presented experimental as well as numerical results for turbine with two adjacent nozzles with 45^{o} apart. The purpose was to also understand the effect of two adjacent nozzles on the performance of the turbine. Figure 4 (i), shows the variation of total pressure for different inlet pressures for 10000 and 40000 rpm. We observe that back nozzle, N2 (Fig. 1 (i)), achieves more velocity than front nozzle N1

with more total pressure drop. Clearly the performance of the back nozzle, N2, drops due to effect of front nozzle, N1. For the same size, contour and inlet pressure of the nozzles, performance of the nozzle N2 significantly drops, which affects the overall efficiency of the turbine.

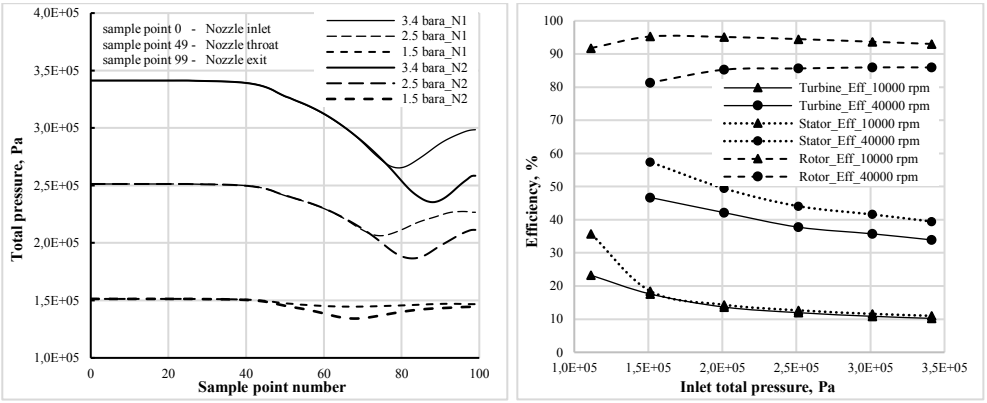

(i) (ii)

Fig. 4. Numerical results ; (i) Variation of total pressure across length of the nozzle ; (ii) Total to static efficiency versus inlet total pressure of turbine for different components

Figure 4 (ii) shows the influence of stator and rotor on the complete turbine performance. Rotor efficiency is calculated using Euler's equation for impulse turbine in which we obtain efficiency by dividing net specific work performed on turbine by fluid to the inlet specific work provided at rotor inlet. The specific work is obtained by multiplying tangential fluid velocity with disk speed. Rotor efficiency is higher in case of lower rotational speed. This could be due to following reason: In case of higher rotational speed of disk, exit fluid velocity of the disk is high. This is the loss of kinetic energy. This loss in kinetic energy makes rotor efficiency at higher rotational speeds lower.

3.2 Turbine M3

In this section, we present the numerical results of M3 turbine with its predicted performance maps. The focus here is to predict the performance of the turbine which is improved using the understanding of mechanism of losses in M02 turbine. Figure 5 shows the performance of the turbine evaluated numerically for 8 nozzles configuration. Peak efficiency of 58% is predicted for 2 bar inlet pressure and at rotational speed of 30000 rpm. We observe that turbine efficiency is high at higher rotational speeds. The peak of an efficiency shifts from lower mass flow and low rpm to high mass flow and high rpm. At higher rotational speeds the efficiency curves become flat which gives us broad operating range. Numerical results do not include different losses mentioned in above section which changes the efficiency trend drastically. Figure 5(ii) shows mechanical power obtained numerically versus mass flow through turbine. Power curves follows similar trend as mentioned in the literature. Power curve becomes more steeper at higher rotational speeds.

The higher efficiency of this turbine is due to following design improvements: (a) Convergent nozzle which keeps the flow subsonic; (b) clearance profile between stator and rotor gap to reduce viscous shear losses; (c) improved nozzle design to minimize total pressure drop; (d) optimized radius ratio for disks (ratio of disk outer radius to disk inner radius). The future work is to characterize M3 turbine losses based on numerical and

experiment results and to study the performance of the turbine by running more design of experiments. The preliminary experimental results for M3 turbine are reported in the paper by Renuke et al [10].

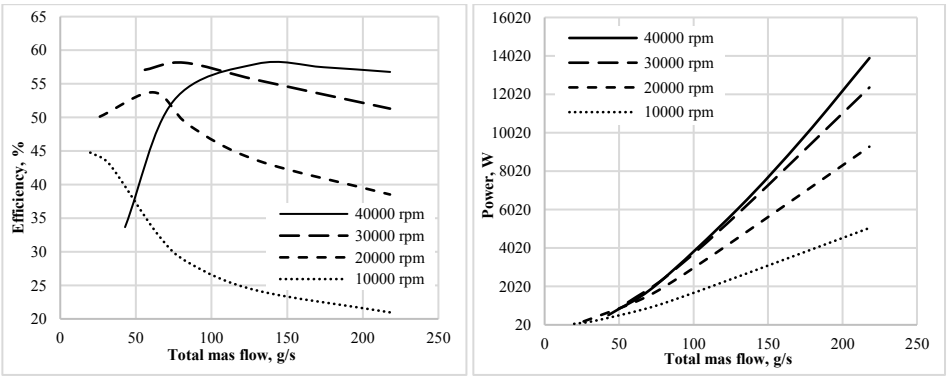

(i) (ii)

Fig. 5. Numerical performance maps for M3 turbine: (i) Efficiency versus total mass flow; (ii) Mechanical power versus total mass flow, at different rotational speeds

4 Conclusions

This paper summarizes comparison and validation of numerical model with experimental results for M02 (200W) and M3 (3 kW) turbines. There is good agreement between CFD model and experimental data. The numerical results are used to understand the low performance of the Tesla expander. The performance of both types of nozzles, Convergent-Divergent (CD) nozzles in M02 turbine and Convergent only nozzle in M3 turbine, reveals that CD nozzles have more total pressure losses due to presence of shock waves. There is a significant effect of multiple nozzles on the performance of turbine which must be studied, and number of nozzles selection must be done carefully. Study reveals that the nozzle contributes to the major losses in the Tesla expander. Moreover, ventilation and bearing losses also contribute in a significant way to lower the performance of turbine. The validation of CFD results gives us an opportunity to use it to optimize the turbine and characterize the losses.

This project has received funding from the European Union's Horizon 2020 research and innovation programme under grant agreement No 764706, PUMP-HEAT.

References

1. Renuke, A., Vannoni, A., Traverso, A., and Pascenti, M., 2019, "Experimental Investigation of Tesla Micro Expanders", *Proceedings: ASME TurboExpo'19*, Phoenix, USA
2. Tesla, N., 1913, "Turbine", US Patent 1061206.
3. Tesla, N.,1913, "Fluid propulsion", US Patent 1061142.
4. Ladino, A.F.R, 2004, "Numerical simulation of the flow field in a friction–type turbine (Tesla turbine)", M.Sc. Thesis, Vienna University of Technology.
5. Lemma, E., Deam, R.T., Toncich, D., and Collins, R., 2008, "Characterization of a small viscous flow turbine", in: Experi-mental Thermal and Fluid Science, 33, 96–105.
6. Lampart, P., Kosowski, K., Piwowarski, M., and Jedrzejewski, L., 2009, "Design analysis of Tesla micro–turbine operating on a low–boiling medium", in: Polish Maritime Research, 28–33.
7. Rusin, K., Wróblewski, W., and Strozik, M., 2018, "Experimental and numerical investigations of Tesla turbine", Journal of Physics, Conf. Series 1101 (2018) 012029.

8. Qi, W., Deng, W., Chi, Z., Hu, L.,Yuan, Q., and Feng, Z., 2019, "Influence of Disc Tip Geometry on the Aerodynamic Performance and Flow Characteristics of Multichannel Tesla Tur-bines", Energies,12,572.
9. Rice, W., 1965, "An Analytical and Experimental Investigation of Multiple Disk Turbines", Journal of Engineering for Power, Vol. 87(1), pp. 29–36
10. Renuke, A., Traverso, A., and Pascenti, M., 2019, "Experimental Campaign Tests on a Tesla Micro-Expanders", SUPEHR'19, Savona, Italy.